

**Table 2**  
Peri-articular bone measures are different among knees with increasing medial meniscal maceration regions

	Medial Meniscal Maceration			p-values		
	0 (N = 389)	1 (N = 45)	2/3 (N = 30)	Overall	Individual Comp. (Tukey Adj.)	
				AN OVA	Ov. 1	1 v. 2/3
Age (years)	63.47 (± 9.16)	67.76 (± 7.49)	65.40 (± 10.13)	0.008	0.01	0.51
BMI (kg/m <sup>2</sup> )	29.53 (± 4.65)	29.53 (± 4.79)	28.95 (± 4.22)	0.80	N/A	N/A
Systemic BMD	0.96 (± 0.14)	0.99 (± 0.17)	1.01 (± 0.18)	0.11	N/A	N/A
M:L paBMD	1.10 (0.14)	1.23 (0.14)	1.24 (± 0.18)	<0.0001	<0.0001	0.99
a. BV/TV	0.10 (± 0.06)	0.15 (± 0.09)	0.15 (± 0.10)	<0.0001	<0.0001	0.99
a.Tb.N (mm <sup>-1</sup> )	0.75 (± 0.35)	1.01 (± 0.36)	0.99 (± 0.42)	<0.0001	<0.0001	0.96
a.Tb.Th (mm)	0.12 (± 0.02)	0.14 (± 0.03)	0.14 (± 0.03)	<0.0001	<0.0001	0.99
a.Tb.Sp (mm)	1.78 (± 1.40)	1.08 (± 0.61)	1.14 (± 0.62)	0.0003	0.005	0.98

maceration in 2 and 3 regions, we collapsed these two groups into one. For ANOVAs that were statistically significant, individual pairwise comparisons with Tukey adjustments were performed on each set of adjacent cells (i.e. 0 vs. 1, 1 vs. 2/3).

**Results:** Among 464 knees, 114 (25%) knees had no medial meniscal pathology, 350 (75%) knees had medial meniscal pathology; including 75 (16%) knees with medial meniscal maceration in at least one region. Knees with medial meniscal pathology were older and had peri-articular medial tibiae with greater M:L paBMD, a.BV/TV, a.Tb.N, and a.Tb.Th compared to knees without medial meniscal pathology (Table 1). Those knees with more medial meniscal maceration regions had similar findings in the peri-articular medial tibia including greater M:L paBMD, a.BV/TV, a.Tb.N, and a.Tb.Th; also the a.Tb.Sp was lower (Table 2).

**Conclusions:** The presence of medial meniscal pathology is associated with peri-articular bone measures in the medial tibia that could be consistent with remodeling or microtrauma. Medial meniscal pathology may lead to periarticular bone changes. Longitudinal studies of earlier OA are needed to test this possibility.

**359**  
**3D FEATURE SEVERITY MAPPING OF THE HIP WITH COMPUTED TOMOGRAPHY REVEALS PATTERNS OF RADIOLOGICAL OSTEOARTHROSIS**

T.D. Turmezei<sup>†</sup>, D.J. Lomas<sup>†</sup>, M.A. Hopper<sup>‡</sup>, K.E. Poole<sup>†</sup>. <sup>†</sup>Univ. of Cambridge, Cambridge, United Kingdom; <sup>‡</sup>Cambridge Univ. Hosp. NHS Fdn. Trust, Cambridge, United Kingdom

**Purpose:** Radiographs are limited in the assessment of hip osteoarthritis by their 2D planar output, which can overlook early disease features and their overall 3D distribution. We present a new approach

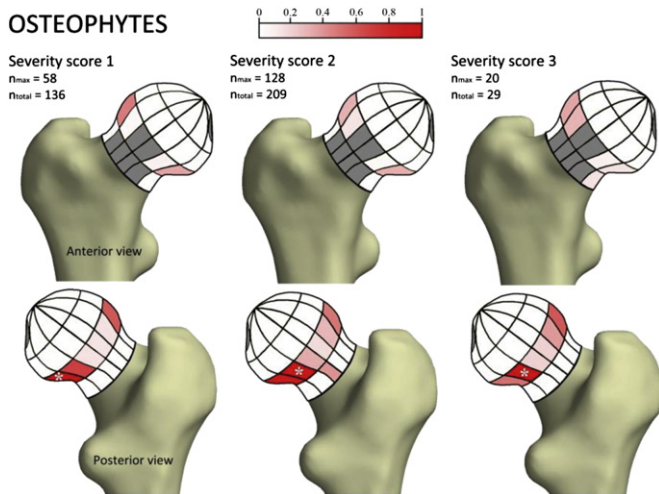


**Figure 1.** 3D feature severity mapping of the proximal femur for osteophyte severity scores 1-3. Sectors in grey were excluded from the analysis (fovea and anterior reaction area). Only the most severe feature score from each hip contributes to the maps according to its severity,  $n_{max}$  = the number of hips in the most frequent sector for a given score (asterisk),  $n_{total}$  = the total number of hips with that score. Sectors are shaded from white to red as a proportion of the  $n_{max}$  sector, thus representing the severity distribution in 3D. An additional 82 hips had a severity score of 0.

to assessing bony features of hip osteoarthritis with computed tomography (CT), a process we have called 'feature severity mapping'.

**Methods:** Clinical CT imaging of 456 hips from 230 female volunteers (mean age 66±17 yrs) were reviewed with standardised multiplanar reformats to record osteophytes, subchondral cysts and joint space width (JSW). A single reviewer used a novel topographic score-sheet to register the location and severity of each feature (scored 0-3). After data collection, a cumulative 3D 'feature severity map' of the proximal femur was created to display the locations of most severe scores from each individual.

**Results:** Osteophytes (definite in 52.2%) occurred most frequently at the inferoposterior and superolateral femoral head-neck junction across all scores (figure 1).

Subchondral cysts (definite in 15.8%) were less common and more scattered. Categorical JSW <1.5mm was recorded in at least one sector of 82.9% of hips, most frequently in the posterior joint space.

**Conclusion:** This 3D analysis sheds new light on key regions of disease in hip osteoarthritis. Frequent osteophyte occurrence at the superolateral femoral head-neck junction corresponds with an established site of impingement-related degeneration. Concordance of osteophyte and joint space narrowing predominance at the posterior joint is a new finding that suggests this region is important in disease development. Further investigation is required to elucidate the biomechanical mechanisms responsible for these findings. This work has also provided the foundation for the development of a novel CT grading system for hip osteoarthritis.

**360**  
**THE DEVELOPMENT AND RELIABILITY OF A NEW CT GRADING SYSTEM FOR HIP OSTEOARTHROSIS**

T.D. Turmezei<sup>†</sup>, D.J. Lomas<sup>†</sup>, M.A. Hopper<sup>‡</sup>, K.E. Poole<sup>†</sup>. <sup>†</sup>Univ. of Cambridge, Cambridge, United Kingdom; <sup>‡</sup>Cambridge Univ. Hosp. NHS Fdn. Trust, Cambridge, United Kingdom

**Purpose:** Clinical trials are in desperate need of imaging biomarkers that can predict the onset and progression of osteoarthritis (OA). While MRI has advantages in the assessment of soft tissue components and radiography is more easily accessible, computed tomography (CT) has the potential to detect bony features of disease in 3D with greater sensitivity and accuracy. Here we present the construction, reliability and disease prevalence from a new CT grading system of hip OA.

**Methods:** In a previous study, we had developed a CT method for 3D mapping of radiological OA features from the multiplanar assessment of 456 hips in 230 female participants (mean age 66±17 yrs). We subsequently created a novel composite hip OA score (0-7) from a weighted interpretation of disease features: osteophytes (0-3), subchondral cysts (0-1), and JSW (0-3). A hip OA grading system was then derived from the composite score (0-2 = 'none'; 3-4 = 'developing'; 5-7 = 'established').

We performed a reproducibility study to test reliability, with two observers assessing 30 anonymised cases (60 hips in total), re-randomised and re-assessed after a 1-month interval. Intra- and inter-observer weighted kappa and overall percentage agreement were calculated for feature scores, composite score and final grade. Disease prevalence was calculated according to the rate of 'established' grade per individual (out of 456) and per hip (out of 230).

**Results:** Intra-observer weighted kappa statistic (95% CI) was substantial for both composite OA score (0.76, 0.48-1.00) and OA grade

	Intra-observer reliability			Inter-observer reliability		
	W kappa (95% CI)	% agreement all scores	% agreement scores 0 vs >0	W kappa (95% CI)	% agreement all scores	% agreement scores 0 vs >0
<b>Osteophytes</b>						
(0-3)	0.78 (0.51-1.00)	91.7%	96.7%	0.62 (0.39-0.86)	71.7%	80.0%
Cysts (0-1)	1.00 (0.91-1.00)	100%	100%	1.00 (0.91-1.00)	100%	100%
<b>JSW</b>						
(0-3)	0.63 (0.35-0.90)	71.7%	81.7%	0.34 (0.06-0.62)	45.0%	58.3%
<b>Composite score</b>						
(0-7)	0.76 (0.48-1.00)	71.7%	81.7%	0.65 (0.41-0.89)	66.7%	66.7%
<b>Grade</b>						
('none', 'developing', 'established')	0.77 (0.56-0.98)	88.3%	95.0%	0.64 (0.43-0.85)	81.7%	86.7%

(0.77, 0.56-0.98). Inter-observer reliability was also substantial for composite score (0.65, 0.41-0.89) and grade (0.64, 0.43-0.85). The least reliable feature was JSW, with an inter-observer weighted kappa of 0.34 (0.06-0.62). Percentage agreement across all grades was 88.3% for reviewer 1 and 81.7% between reviewers. Full results are given here: The prevalence of 'established' hip osteoarthritis in this cohort was 8.3% by individual and 4.8% by hip, comparing favourably to reported disease prevalence of 5-7% in women of a similar age range from other epidemiological studies.

**Conclusion:** This new CT grading system shows substantial reliability in the assessment of hip osteoarthritis. The composite scoring system also shows substantial reliability and has the potential to offer greater sensitivity in disease assessment, as well as the ability to categorise atrophic, normotrophic and hypertrophic phenotypes according to score breakdown. Further testing will be performed in a prospective setting against the outcome of total hip replacement to test construct validity. 5 year follow-up imaging will also be used to test construct sensitivity.

### 361 FLUORESCENCE REFLECTANCE IMAGING OF EARLY PROCESSES OF POST-TRAUMATIC OSTEOARTHRITIS IN MALE AND FEMALE MICE

P.B. Satkunananthan, M.J. Anderson, N. De Jesus, C.M. Ripplinger, B.A. Christiansen. UC Davis Med. Ctr., Sacramento, CA, USA

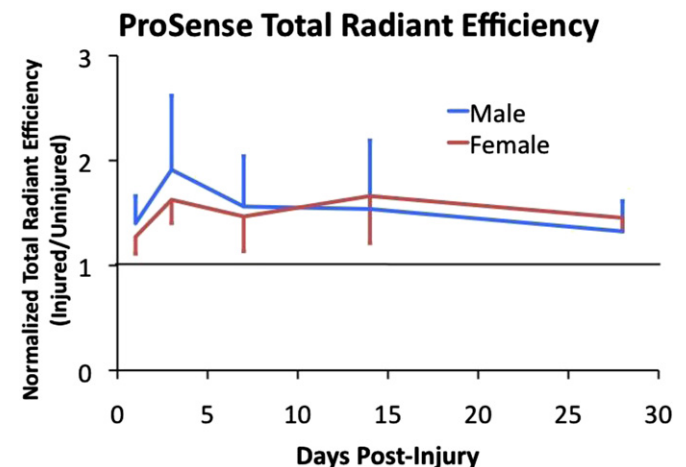
**Purpose:** Approximately 50% of individuals that experience anterior cruciate ligament (ACL) rupture develop post-traumatic osteoarthritis (PTOA) within 10-20 years, resulting in severe joint pain and stiffness. Although females are 4-6 times more likely than males to sustain an ACL injury during exercise or sports, males demonstrate an increased tendency to develop osteoarthritis following injury. ACL rupture initiates a surge of inflammatory cytokines, matrix metalloproteinases (MMPs), and other proteases, as well as cartilage degeneration and rapid bone turnover. It is possible that the magnitude or time course of these early biological responses may differ by sex, making males more likely to develop PTOA, however the quantification of these processes in males and females has not been performed. In this study, we used fluorescence reflectance imaging to quantify the time course of the early biological response to traumatic joint injury in male and female mice in vivo using highly sensitive activatable fluorescent agents that quantify protease activity, MMP activity, and osteoclastic bone resorption in injured and uninjured knees.

**Methods:** A total of 48 mice were subjected to non-invasive knee injury as previously described (Christiansen et al., Osteoarthritis and Cartilage, 2012). Three groups of 16 mice (8 male, 8 female) were imaged with either ProSense 680, MMPsense 680, or CatK 680 FAST (Perkin Elmer, Waltham, MA) in order to quantify protease activity, MMP activity, or osteoclastic bone resorption, respectively. Injections were administered 24-30 hours prior to imaging, on days 1, 3, 7, 14, 21, 28, and 56 after initial injury. At each time point of interest, mice were anesthetized with isoflurane, and imaged with the IVIS Spectrum system. Fluorescent signals were quantified by evaluating radiant efficiency of the signal within a uniform region of interest (ROI), anatomically selected around the knee on grayscale photograph. Radiant efficiency of the injured knee was normalized by that of the contralateral uninjured knee.

**Results:** For both male and female mice, protease activity (ProSense), MMP activity (MMPsense), and osteoclastic bone resorption (CatK) were significantly increased in the injured knee relative to the

uninjured knee at nearly all time points. For example, Protease activity was significantly increased by day 1, reached a peak between 3 and 14 days, then decreased at later time points (Figure). Males and females displayed similar changes in injury response through the time periods observed, with males averaging a slightly higher normalized radiant efficiency at early time points, although this was not statistically different.

**Conclusions:** Using commercially available activatable fluorescent agents, we were able to quantify the time course of protease activity, MMP activity, and osteoclastic bone resorption in male and female mice following traumatic knee injury. However, contrary to our hypothesis, we were not able to observe a significant differential response between male and female mice. Our future studies will continue to explore potential mechanisms of the sex-based adaptation to joint injury that may contribute to the greater incidence of PTOA development in males. Our future studies will also continue to use fluorescence reflectance imaging as a method for measuring biological activity in vivo.



### 362 T2\* OF CALCIFIED CARTILAGE AND OSTEOCHONDRAL JUNCTION AT 3 TESLA AND 7 TESLA FIELD STRENGTH AND HISTOLOGICAL CORRELATION

M.I. Menendez<sup>1,2,3</sup>, V. Juras<sup>4</sup>, J. Hofstaetter<sup>5</sup>, M. Brix<sup>6</sup>, S. Walzer<sup>7</sup>, P. Szomolanyi<sup>8</sup>, O. Bieri<sup>9</sup>, X. Deligianni<sup>10</sup>, S. Trattnig<sup>11</sup>. <sup>1</sup>The Wright Ctr. of Innovation in BioMed. Imaging, The Ohio State Univ. Wexner Med. Ctr., Columbus, OH, USA; <sup>2</sup>Coll. of Vet. Med., The Ohio State Univ., Columbus, OH, USA; <sup>3</sup>MR Ctr. of Excellence, Dept. of Radiology, Med. Univ. of Vienna, Vienna, Austria; <sup>4</sup>Dept. of Orthopaedics, Med. Univ. of Vienna, Vienna, Austria; <sup>5</sup>Dept. of Radiology and Nuclear Med., Univ. of Basel Hosp., Basel, Switzerland

**Purpose:** Understanding the pathophysiology of osteoarthritis (OA) requires a clear definition of the tissues underneath the articular cartilage, including the osteochondral junction (OJ) or tidemark and calcified cartilage (CC). Calcified cartilage begins to advance into the